# 83885\_Auto\_Edited.docx

#### Analysis of N6-methyladenosine-modified mRNAs in diabetic cataract

Cai L et al. M6A-modified mRNAs in DC

Lei Cai, Xiao-Yan Han, Dan Li, Dong-Mei Ma, Yu-Meng Shi, Yi Lu, Jin Yang

#### **INTRODUCTION**

Over the last several decades, the prevalence of diabetes mellitus (DM) in adults has increased globally. There were approximately 110 million DM cases in China in 2015, and the number is estimated to be 150 million by 2040, as indicated by the International Diabetes Federation<sup>[1]</sup>. DM, a systemic condition, affects various organs and thus can induce several complications, including cataracts<sup>[2]</sup>. Despite the increasing maturity of modern cataract surgery technology, cataracts remain a prime reason for vision loss and blindness globally<sup>[3,4]</sup>. Diabetic cataracts (DCs) usually develop at an earlier age and progresses more rapidly than age-related cataracts do<sup>[5]</sup>. Evidence has linked DC to polyol pathway, nonenzymatic glycation, and oxidative stress (OS)<sup>[4]</sup>. Yet, the molecular mechanism underlying DC progression remains largely unknown.

As environmental factors play critical roles in the pathogenesis of DM, epigenetic changes may be particularly important<sup>[6]</sup>. N6-methyladenosine (m6A), one of the most prevalent epigenetic modifications in mammals<sup>[7]</sup>, is increasingly shown to be crucial in several pathological processes (*e.g.*, tumorigenesis, angiogenesis, tissue degeneration, and inflammatory responses)<sup>[8,9]</sup>. A study on DC pathogenesis based on m6A-RNA immunoprecipitation (MeRIP)-sequencing reported that the level of the methyltransferase protein complex, methyltransferase-like 3 (METTL3), is upregulated in high glucose-induced human lens epithelial cells (LECs) and that METTL3 mediates a higher methylation level<sup>[10]</sup>. However, the RNA m6A modification landscape in DC and the role of m6A in DC pathogenesis are still largely undetermined.

Herein, we performed an m6A epitranscriptomic microarray analysis to identify differentially methylated mRNAs and determined their potential roles using

bioinformatics analyses, rendering novel insights into the pathogenic mechanisms of DC as well as clues for future biological interventions.

#### **MATERIALS AND METHODS**

#### Participants and specimen collection

The anterior lens capsule (ALC) tissue of three DC patients had been living with diabetes for more than 5 years was collected, and the cataract severity was graded using the Lens Opacities Classification System III<sup>[11]</sup>. In addition, ALCs collected from agematched transparent crystals of cadaveric eyes were used as normal controls (NC). Patients with other eye diseases, such as high myopia, trauma, uveitis, or glaucoma were excluded from the study. Patients' information is presented in Table 1. The workflow of sample collection and processing is shown in Figure 1. This study has obtained approval from the Ethics Committee of the Eye and ENT Hospital of Fudan University and written informed consent from all participants, and the principles of the Declaration of Helsinki were strictly follows throughout the research period. This study was registered with ClinicalTrials.gov, number NCT05682001.

#### Cell culture

The human LEC line SRA01/04, obtained from Genechem, was immersed in Dulbecco's modified Fagle's medium (Thermo Fisher Scientific, United States) where 5.5 mmol/L glucose, 10% fetal bovine serum (Invitrogen, Carlsbad, CA, United States), 100 IU/mL penicillin (Thermo Fisher Scientific), and 100 mg/mL streptomycin (Thermo Fisher Scientific) were added, for cultivation in a 5% CO<sub>2</sub> humidified atmosphere with the temperature maintained at 37 °C. Confluent cells (75%-80%) were then randomly grouped as a normal- (NG group; 5.5 mmol/L glucose-supplemented medium) and a high-glucose group (HG group; 25.0 mmol/L glucose-supplemented medium), and cultured for 24 h for subsequent examinations.

#### Total RNA extraction and m6A immunoprecipitation

Using TRIzol (Invitrogen) and following kit recommendations, total RNA was isolated from the LECs of the included DC patients and controls, as well as SRA01/04 cells, followed by RNA quantification and purity evaluation with a NanoDrop ND-1000 spectrophotometer purchased from Thermo Fisher Scientific. This was followed by immunoprecipitation (IP) of the extracted total RNA from the NC (n = 3) and DC samples (n = 3) with an anti-m6A antibody by referring to the manufacturer's recommendations. In brief, we placed 2 µg total RNA and m6A spike-in control mixture into a 300 µL IP buffer supplemented with 2 µg anti-m6A rabbit polyclonal antibody (Synaptic Systems, Goettingen, Germany), and let the reaction mixture rotate headover-tail for 2 h at 4 °C. A DynabeadsTM M-280 sheep anti-rabbit immunoglobulin G (IgG) suspension (20 µL) was blocked with freshly prepared 0.5% bovine serum albumin at 4 °C for 2 h, followed by three rinses with IP buffer (300 µL) and resuspension in the total RNA-antibody mixture prepared. The RNA was then allowed to bind to the m6A-antibody beads for 2 h at 4 °C via head-over-tail rotation. After washing the beads thrice with 500 µL 1 × IP buffer and twice with 500 µL wash buffer, and incubation with 200 µL elution buffer (50 °C, 1 h), the enriched RNA was eluted and extracted using acid phenol-chloroform for ethanol precipitation.

#### Two-color RNA labeling and hybridization

The immunoprecipitated m6A-enriched RNAs were eluted from the magnetic beads as "IP", while the unmodified RNAs were collected from the supernatant as "Sup", which were then labeled with Cy5 and Cy3 (cRNAs), respectively, using an Arraystar Super RNA Labeling Kit (Arraystar, AL-SE-005). Purification of the synthesized cRNAs employed a RNeasy Mini Kit (QIAGEN, 74105), and the determination of concentrations and specific activities used the NanoDrop ND-1000. Following Arraystar's standard protocol, microarray hybridization was performed. We combined and hybridized Cy3 and Cy5 Labeled cRNAs to an Arraystar Human mRNA Epitranscriptomic Microarray (4 × 44 K, Arraystar, China), after which the slices were washed for array scanning using an Agilent Scanner G2505C (Agilent, Beijing, China).

#### Data analysis

Analyses of the acquired array images were carried out using Agilent's Feature Extraction software v11.0.1.1. Cy5-labeled IP and Cy3-labeled Sup raw intensities were normalized to the mean of log2-scaled spike-in RNA intensities. The m6A methylation level was counted as a percentage of modified RNA (% modified) from total RNA, based on IP and Sup normalized intensities. The m6A quantity of each transcript was calculated according to normalized IP (Cy5-labeled) intensities. RNA expression was determined from the total IP and Sup normalized RNA intensities.

#### Gene ontology and pathway analysis

The online gene ontology (GO) (URL: http://www.geneontology.org) and Kyoto Encyclopedia of Genes and Genomes (KEGG) databases (URL: http://www.genome.jp/kegg) were utilized for determining the enriched GO terms and pathways in the mRNAs with significantly different m6A expression levels.

#### MeRIP coupled with real-time quantitative polymerase chain reaction

To validate microarray data quality, MeRIP-quantitative polymerase chain reaction (qPCR) was performed on four randomly selected mRNAs. In brief, the IP RNAs from ALC tissues of patients with DC and NCs were analyzed for microarray data validation, with primers used presented in Supplementary Table 1.

#### Reverse transcription-qPCR

Reverse transcription of total RNA to cDNA was performed as per the instruction of the PrimeScript RT Reagent Kit (Takara, Dalian, Liaoning province, China). Reverse transcription-qPCR (qRT-PCR) primers, designed with the use of Primer 5.0, were blasted for specificity in NCBI (Supplementary Table 1). An Applied Biosystems ViiA 7 Real-Time thermal cycler (Thermo Fisher Scientific) and 2YBR Green PCR Master Mix (Arraystar) were then utilized to perform the qRT-PCR. The expression of target

mRNAs were normalized against Actin, and fold changes were determined by the comparative CT ( $2^{-\Delta\Delta CT}$ ) method.

#### Statistical analysis

The significance threshold was P < 0.05 in this study. For the microarray analysis, statistical significance in methylation levels between DC cases and NCs was identified using an unpaired two-sided t-test. For GO and KEGG analyses, GO terms and KEGG pathway identifiers with significant differences were identified using the Fisher's exact test p-value and -log10(p) transformed as the enrichment score. While the relative genes' expression in MeRIP-qPCR and qRT-PCR was worked out by  $2^{-\Delta\Delta CT}$ .

#### RESULTS

Epitranscriptomic microarray analysis reveals the differential m6A modification of mRNAs in DC samples

Microarray analyses of the mRNAs extracted from the lens anterior capsule tissues of the DC and NC samples showed differential m6A-methylated mRNAs, as identified by the "m6A-mRNA quantity and m6A-mRNA methylation level". The results have been presented as heatmaps (Figure 2A and C) and volcano plots (Figure 2B and D). According to the m6A quantity results, there were 7153 hypermethylated mRNAs and 3667 hypomethylated mRNAs. As per the m6A methylation level results, 1125 mRNAs had higher m6A methylation levels, whereas 220 mRNAs had lower levels. See Table 2 for the top 20 mRNAs with the most significant hyper- and hypomethylation levels between DC cses and NCs.

GO and KEGG pathway analyses reveal the biological function of differentially methylated mRNAs in DC

The enriched GO annotations can be fall into biological process (BP), cellular component (CC), or molecular function (MF). For hypermethylated mRNAs, 580 BPs, 110 CCs, and 100 MFs were enriched. The quantity of differentially methylated mRNAs

related to the listed GO ID was recorded; of them, the top 10 most significantly enriched terms are presented as pie charts (Figure 3A-C, G). In addition, the top four terms with the highest enrichment score are shown in Figure 3G. For the hypomethylated mRNAs, 288 BPs, 47 CCs, and 67 MFs were enriched. See Figures 3D-F and 3H for the top 10 most significantly enriched terms and the top 4 terms with the highest enrichment scores.

Based on KEGG pathway analysis, the mRNAs differentially methylated by m6A participated in 27 pathways (Figure 4A and B). Most of the hypermethylated mRNAs were primarily enriched in "ferroptosis", "PPAR axis", and "alpha-linolenic acid metabolism". The ferroptosis pathway map is illustrated in Figure 4C.

#### Functional analysis of differentially expressed mRNAs in DC specimens

Besides m6A modification levels, the m6A microarray analyses provided data for mRNA expression (Figure 5A and B). A total of 12015 mRNAs in the DC and NC groups showed significantly different expression [ $P \le 0.05$ , fold change (FC)  $\ge 1.5$ ], 7698 of which were upregulated, whereas 4317 were downregulated. The functions of the top 20 differentially expressed mRNAs (DEmRNAs) (Supplementary Table 2) were analyzed using GO and KEGG pathway analyses. Among the enriched GO terms, 780 BPs, 137 CCs, and 101 MFs were associated with downregulated mRNA expression, with the top 10 displayed in Figure 5C. Moreover, 1199 BPs, 119 CCs, and 190 MFs were identified to be linked to upregulated mRNA expression, with the top 10 presented in Figure 5D. Among the upregulated mRNAs of the BP category, "cellular component organization" had the highest GO term enrichment score, whereas for the downregulated mRNAs, the highest score belonged to "positive regulation of immune effector process". For the CC category, "intracellular" and "plasma membrane" were the most prominent GO terms for up- and down-regulated mRNA expression, respectively. In the MF category, "protein binding" was the most significant term for both up- and downregulated mRNAs.

According to KEGG pathway analysis, DEmRNAs participated in 55 pathways, most of which were primarily enriched in the "MAPK axis", "Type II DM", and "cAMP axis" (Figure 5E and F).

#### Combined analysis of m6A methylation and mRNA expression in DC samples

Using the thresholds  $FC \ge 1.5$  and  $P \le 0.05$ , the combined analysis revealed significantly altered m6A methylation and mRNA expression levels in 1,320 mRNAs. Conjoint analysis of these 1320 mRNAs resulted in the formation of four mRNA groups: Group I, 958 hypermethylated and upregulated mRNAs; Group II, 105 hypermethylated and downregulated mRNAs; Group III, 207 hypomethylated and downregulated mRNAs; Group IV, 50 hypomethylated and upregulated mRNAs (Figure 6A). Several key genes of ferroptosis (*PRNP*, *SLC39A8*, *VDAC2*, *P53*, *CYBB*, *ATG7*, and *SLC3A2*) were found in Group I.

Hypermethylated-upregulated (hyper-up) and -downregulated (hypo-down) mRNAs were further identified using GO and KEGG pathway analyses. For Group I mRNAs, the most enriched GO terms in BP, CC, and MF categories were found to be "protein membrane anchor", "early phagosome", and "sodium ion binding", respectively. For Group III mRNAs, the terms were "lens fiber cell development", "cohesin complex", and "translation release factor activity binding" (Figure 6B). KEGG pathway analysis showed that DEmRNAs participated in 26 pathways. Most mRNAs in Group I were mainly enriched in "alpha-linolenic acid metabolism," "ferroptosis", and "apoptosis", whereas Group III mRNAs were primarily enriched in "calcium axis", "cGMP-PKG axis", and "tight junction" (Figure 6C and D).

## Validation of the diverse methylated mRNA and RNA methyltransferase expression patterns in vivo and in vitro

We randomly selected four mRNAs (BECN2, METTL21A, NFE2, and TIPRL) for MeRIP-qPCR to validate the microarray data quality; specifically, we screened the differentially methylated mRNAs under the criteria of P value  $\leq 0.05$  and  $FC \geq 1.5$ , and

then we selected genes with multiple expression folds for verification with the primers can be designed for those mRNAs. Finally, we selected 4 methylated mRNAs with different fold changes for verification to ensure the reliability of the results to a certain extent. Details of the selected genes are listed in Supplementary Table 3), and the results accorded with the microarray data (Figure 7A). Furthermore, to explore the possible genes participating in m6A modification, we compared the expression of the DEmRNAs in our epitranscriptomic\_microarray with that of 24 known methylationrelated genes (METTL3, METTL14, WTAP, VIRMA, KIAA1429, RNA binding motif protein 15 (RBM15), RBM15B, ALKBH5, FTO, AlkB-H9, HNRNPA2, HNRNPB1, HNRNPC1, HNRNPC2, YTHDC1, YTHDC2, YTHDF1, YTHDF2, YTHDF3, EIF3A, EIF3B, IGF2BPs, DGCR8, and ELAVL1). The expression of five genes (RBM15, WTAP, ALKBH5, FTO, and YTHDF1) was found to be upregulated in the microarray results (Figure 7B; the FC values of these genes are shown in Figure 7C); and of these, RBM15 exhibited the highest change in expression level. Additionally, the upregulation of RBM15 in SRA01/04 cells cultured in HG medium verified its expression in vitro, supporting the qRT-PCR results in DC specimens (Figure 7D).

#### DISCUSSION

The present study elucidated the m6A landscape in DC using an epitranscriptomic microarray, which simultaneously analyzed the methylation and expression of related mRNA. According to the microarray results, a total of 1345 mRNAs exhibiting significantly different m6A modification levels between DC cases and NCs were identified. Most of these mRNAs (1125/1345) had higher m6A methylation levels in the DC samples. First identified in the 1970s, abundant m6A modifications in polyadenylated RNA were accidentally discovered by some research groups when they were characterizing the 5' structures of mRNA in mammalian cells<sup>[12]</sup>. In multiple human pathophysiological processes, m6A extensively modifies RNA transcription and protein generation<sup>[13]</sup>. Modification by m6A modulates gene expression by affecting mRNA splicing, localisation, stability, and translation. Over the past few years, the

development of techniques such as MeRIP-sequencing and epitranscriptomic microarrays has made the high-throughput measurement of m6A modification sites possible<sup>[14-16]</sup>. These approaches allow simultaneous screening of modified transcript types and modification changes under different conditions, as well as detection of modification proportions per transcript. The development of microarray method has allowed for a more subtle mapping of the m6A modification, providing better insights into its importance in gene regulation.

In this study, RBM15 was found most upregulated in the DC group, which was verified in DC samples and HG-cultured LECs. Methylation through m6A is a reversible process, dynamically regulated by three different types of protein complexes: methyltransferases, demethylases, and readers<sup>[17]</sup>. RBM15 and its paralog, RBM15B, are additional components of the methyltransferase complex<sup>[18]</sup>. RBM15, a split-end protein family member, modulates m6A methylation for RNA modification<sup>[19]</sup>. As part of the methyltransferase complex, it participates in hematopoietic cell homeostasis and alternative mRNA splicing<sup>[20]</sup>. The main role of RBM15 in m6A methylation catalysis is recruiting the m6A methyltransferase complex to U-rich regions adjacent to m6A sites[18,21]. Pollreisz et al[22] reported markedly increased global mRNA m6A methylation level and RBM15 expression in laryngeal squamous cell cancer patients; however, inhibiting RBM15 led to a notable reduction in the m6A methylation level. But the potential roles played by RBM15 in DC pathogenicity need further research. It could be suggested that RBM15-mediated m6A modification of LECs may promote DC progression. Further studies are warranted to clarify the mechanisms underlying m6A modification in DC.

Further, based on the KEGG pathway analysis, ferroptosis was identified as one of the most enriched pathways in the m6A-hypermethylated and upregulated mRNAs in DC samples (Figure 4C). In human lens development, LECs play a key role in transport, metabolism, and detoxification<sup>[23]</sup>. The integrity and survival of LECs are critical for lens transparency<sup>[24]</sup>. LEC death due to apoptosis and autophagy plays pathophysiological roles in DC progression<sup>[25]</sup>. Ferroptosis is a newly defined

programmed death mode that is implicated in various reactive oxygen species (ROS)-related pathophysiological states, such as age-related macular degeneration and cardiovascular diseases<sup>[26,27]</sup>. OS is vital in DC pathogenesis<sup>[28]</sup>. The process of ferroptosis is characterized by glutathione (GSH) depletion, lipid peroxidation, and intracellular ROS accumulation with iron overload as well as accelerated cell death<sup>[29-31]</sup>. GSH levels are markedly lower in DC patients than in non-diabetic senile cataract patients and non-diabetic type 2 DM patients as well as in healthy individuals<sup>[32]</sup>.

The subsequent combined analysis of m6A methylation and mRNA expression levels showed several ferroptosis-associated key genes (PRNP, SLC39A8, VDAC2, P53, CYBB, ATG7, and SLC3A2) to be hypermethylated and upregulated in the DC group, suggesting enhanced ferroptosis in LECs of patients with DC. P53 can potentiate ferroptosis by inhibiting the transcription of system xc-subunit SLC7A11<sup>[33]</sup>. Reportedly, its expression was upregulated in the LECs of patients with DC<sup>[34]</sup>. Therefore, we speculate that m6A mRNA modifications of LECs are involved in DC progression *via* the ferroptosis pathway. In future, more comprehensive research is warranted to elucidate ferroptosis-associated mechanisms in DC pathogenesis.

#### **CONCLUSION**

Collectively, the m6A abundance level in total mRNA increased in patients with DC. Conjoint analysis indicated that m6A mRNA modifications of LECs might be involved in DC progression *via* the ferroptosis pathway. The expression level of RBM15 increased, which provided a better understanding of the mechanisms underlying upregulated m6A demethylation levels.

#### **Figure Legends**

**Figure 1 Workflow of the experimental design.** m6A: N6-methyladenosine; QC:

#### Figure 2 Microarray data analysis showing expression profile of methylated mRNAs.

A: Visualization of differential N6-methyladenosine (m6A) quantity profiles of mRNAs between the diabetic cataract (DC) and normal control (NC) groups through heat map and hierarchical clustering, where red and green colors indicate up- and down-regulated mRNAs, respectively; B: Volcano plot showing significant dysregulation of 10820 (7153 upregulated and 3667 downregulated) mRNAs in DC cases compared to NCs; C: Visualization of differential m6A mRNA methylation level profiles between DC cases and NCs through heat map and hierarchical clustering, where red and green colors indicate up- and down-regulated mRNAs, respectively; D: Volcano plot showing significant dysregulation of 1345 (1125 upregulated and 220 downregulated) methylated mRNAs in DC cases versus NCs.

Figure 3 Overall distribution of Gene Ontology analysis. A-C: The hypermethylated mRNAs were categorized into biological process (BP), cellular component (CC), or molecular function (MF). Of the Gene Ontology (GO) terms significantly enriched, 580 BPs, 110 CCs, and 100 MFs had higher mRNA methylation levels; D: The top four most enriched GO terms of the hypermethylated mRNAs; E-G: Classification of hypomethylated mRNAs in the BP, CC, and MF categories. For the hypomethylated mRNAs, 288 BPs, 47 CCs, and 67 MFs were identified; H: The top four most enriched GO terms of the hypomethylated mRNAs.

Figure 4 Kyoto encyclopedia of Genes and Genomes pathway analysis. A: The top 10 Kyoto Encyclopedia of Genes and Genomes (KEGG) pathways of hypermethylated mRNAs; ferroptosis is the most enriched axis; B: The top 10 KEGG pathways of hypomethylated mRNAs; C: Please add subtitle.

Figure 5 Microarray data showing the profiles of differentially expressed mRNAs. A: Visualization of differentially expressed mRNAs (DEmRNAs) profiles between diabetic cataract (DC) cases and normal controls (NCs) through heat map and hierarchical clustering, where red and green colors indicate up- and down-regulated mRNAs, respectively; B: Volcano plot showing significant dysregulation of 12015 mRNAs in DC cases than in NCs; C and D: The top four most enriched Gene Ontology terms of down-(C) and up-regulated mRNAs (D); E and F: The top 10 Kyoto Encyclopedia of Genes and Genomes pathways of down (E) and up-regulated mRNAs (F).

Figure 6 Combined analysis of N6-methyladenosine methylation and mRNA expression levels. A: Visualization of the positive correlation of differential N6-methyladenosine methylation with differential mRNA expression *via* a four-quadrant graph; B and C: The top four Gene Ontology terms significantly enriched for the hypermethylated-upregulated (hyper-up) genes (B) and the hypomethylated-downregulated (hypo-down) genes (C); D and E: The top 10 Kyoto Encyclopedia of Genes and Genomes pathways significantly enriched for the hyper-up (D) and hypodown genes (E).

Figure 7 Validation of the diverse expression levels of methylated mRNA and RNA methyltransferase, using *in vivo* and *in vitro* models. A: Methylation levels of *BECN2*, *METTL21A*, *NFE2*, and *TIPRL* are consistent with the microarray data for the diabetic cataract and normal control groups; B: Intersection results of upregulated mRNAs and N6-methyladenosine-related genes; C: Fold change values of five genes (*RBM15*, *WTAP*, *ALKBH5*, *FTO*, and *YTHDF1*) in microarray results; D: The mRNA levels of *RBM15* are significantly higher in high-glucose cultured SRA01/04 cells than in normal-glucose cultured ones. SC: Diabetic cataract; NC: Normal control; HG: High-glucose; NG: Normal-glucose. aP < 0.05.

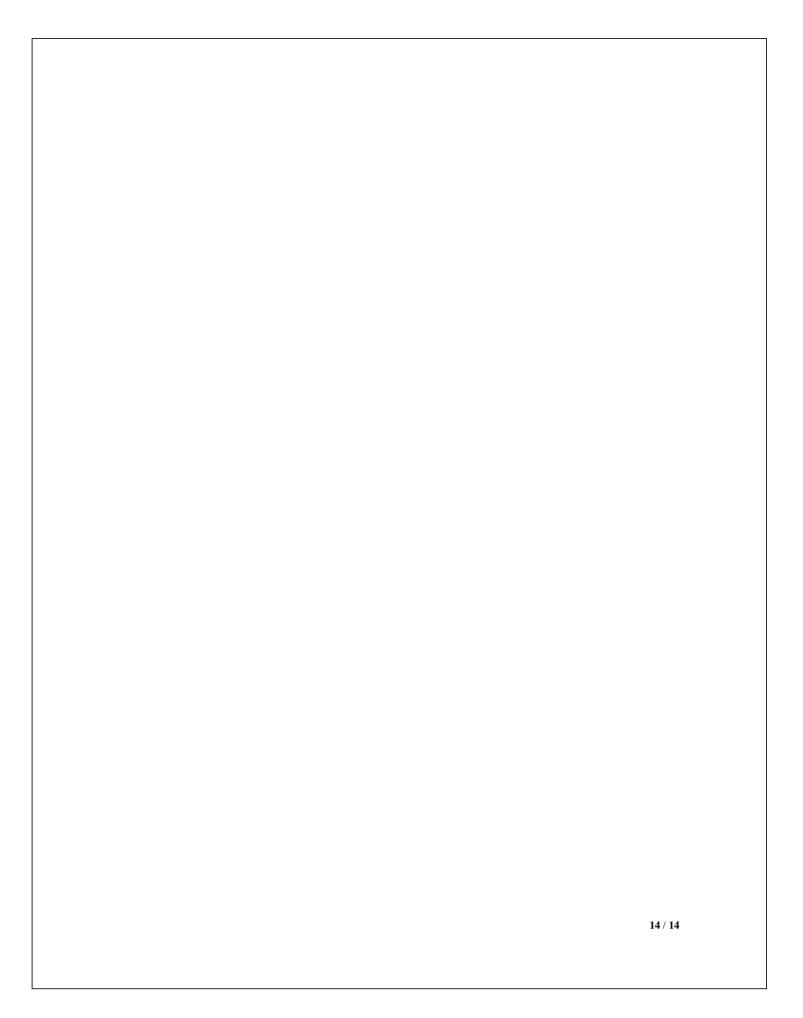
Table 1 Features of diabetic cataract patients included in microarray analysis

No.	Gender	Age	AL	Lens opacity	<b>Puration</b> of	FBG	HbA1c
		(yr)	(mm)	grading	DM (year)	(mmol/L)	(%)
1	Male	64	22.09	C4N3P3	10	7.89	7.50
2	Female	68	21.77	C3N4P4	7	8.30	7.80
3	Female	63	23.43	C4N4P5	7	8.30	7.90

AL: Axial length; FBG: Fasting blooding glucose; HbA1c: Hemoglobin.

Table 2 The top 20 most hyper- and hypomethylated mRNAs

Gene symbol	P value	Fold change	Regulation	Chromosome
AQP2	0.001135123	3.60	hyper	chr12
RPL10	0.001594064	3.40	hyper	chrX
ACP5	0.004544885	3.25	hyper	chr19
ACAP1	0.003944032	3.21	hyper	chr17
CALML6	0.00484061	3.05	hyper	chr1
DDX31	1.02006E-05	3.04	hyper	chr9
KRTAP29-1	3.59728E-05	2.97	hyper	chr17
TRIM39-RPP21	0.001179594	2.95	hyper	chr6
DGCR8	0.013600714	2.90	hyper	chr22
LRAT	0.001067196	2.90	hyper	chr4
NR1H3	0.028959935	5.78	hypo	chr11
PNPT1	0.001479448	4.99	hypo	chr2
TSEN2	0.015094744	4.99	hypo	chr3
C3orf80	0.000939962	4.61	hypo	chr3
TBCD	0.001813039	4.61	hypo	chr17
RPS19	0.004668423	4.12	hypo	chr19
TEAD2	0.031922173	4.02	hypo	chr19
RAB3IP	0.005656491	3.96	hypo	chr12
HN1L	0.008004647	3.77	hypo	chr16
TFEB	0.004349132	3.70	hypo	chr6



## 83885\_Auto\_Edited.docx

**ORIGINALITY REPORT** 

20% SIMILARITY INDEX

**PRIMARY SOURCES** 

- $\frac{\text{www.nature.com}}{\text{Internet}} \qquad \qquad 73 \, \text{words} 2\%$
- $\frac{\text{www.frontiersin.org}}{\text{Internet}} \qquad \qquad \text{65 words} 2\%$
- Xiaoshuai Wang, Ningning Chen, Zefeng Du, Zemin Ling et al. "Bioinformatics analysis integrating metabolomics of m A RNA microarray in intervertebral disc degeneration ", Epigenomics, 2020
- Liangliang Shen, Yue Yu, Miao Jiang, Jingjun Zhao. 
  Alteration of the m A methylation landscape in a mouse model of scleroderma ", Epigenomics, 2021 Crossref
- Xiaoyan Han, Lei Cai, Yumeng Shi, Zhixiang Hua, Yi
  Lu, Dan Li, Jin Yang. "Integrated Analysis of Long
  Non-Coding RNA -mRNA Profile and Validation in Diabetic
  Cataract", Current Eye Research, 2022
- 6 www.ncbi.nlm.nih.gov 52 words 1 %
- Xiaoli Jia, Zhilong Zhang, Rongqiang Wei, Bin Li, Yiyang Chen, Jiang Li. "Comprehensive analysis of 49 words -1%

### transcriptome-wide m6A methylome in intermediate-stage Esophageal squamous cell carcinoma", Pathology - Research and Practice, 2022

Crossref

8	www.spandidos-publications.com  Internet	38 words — <b>1</b> %
9	www.bioseek.eu Internet	24 words — <b>1</b> %
10	portlandpress.com Internet	23 words — <b>1</b> %
11	www.hindawi.com Internet	22 words — <b>1</b> %
12	Xi Shen, Pan Chang, Xiaomeng Zhang, Jing Zhang et al. "The landscape of 6-methyladenosine modification patterns and altered transcript profiles cardiac-specific deletion of natriuretic peptide recept Molecular Omics, 2022  Crossref	

- Yuhao Zhang, Xiuchao Geng, Jianglong Xu, Qiang Li et  $_{21 \text{ words}} 1\%$  al. "Identification and characterization of N6 methyladenosine modification of circRNAs in glioblastoma", Journal of Cellular and Molecular Medicine, 2021  $_{\text{Crossref}}$
- Yingqian Peng, Zicong Wang, Bingyan Li, Wei Tan,  $_{17 \text{ words}} < 1\%$  Jingling Zou, Yun Li, Shigeo Yoshida, Yedi Zhou. "N6-methyladenosine modifications of mRNAs and long noncoding RNAs in oxygen-induced retinopathy in mice", Experimental Eye Research, 2022 Crossref

15	www.researchsquare.com Internet	17 words — <b>&lt;</b>	1%
16	Yuanyuan Zeng, Hengxing Liang, Yue Guo, Yunzh Feng, Qianqian Yao. "Adiponectin regulates osteocytic MLO - Y4 cell apoptosis in a high - glue environment through the AMPK/FoxO3a signaling Journal of Cellular Physiology, 2021 Crossref	cose	1%
17	bsdwebstorage.blob.core.windows.net	16 words — <b>&lt;</b>	1%
18	Zhu Li, Yi Liu, Ling Zhang, Jiahua Tian, Hongping Wang, Hongwei Ding, Jin Nie, Hang Pi, Bingyao Wang, Daishun Liu. "N6-methyladenosine modific contributes to respiratory syncytial virus infection 2023  Crossref		1%
19	www.dovepress.com Internet	12 words — <b>&lt;</b>	1%
20	repository.helmholtz-hzi.de Internet	11 words — <	1%
21	discovery.ucl.ac.uk Internet	10 words — <	1%
22	assets.researchsquare.com	9 words — <b>&lt;</b>	1%
23	kclpure.kcl.ac.uk  Internet	9 words — <b>&lt;</b>	1%

link.springer.com

9 words — < 1 %

- "Epitranscriptomics", Springer Science and Business Media LLC, 2021
- 8 words < 1%

Crossref

- Salgado Albarrán Marisol. "Estudio genómico del factor epigenético boris y su participación en cáncer de ovario", TESIUNAM, 2021
- 8 words < 1%
- Yuwei Wang, Yuhong Chen, Jian Liang, Mei Jiang et al. "METTL3-mediated m6A modification of HMGA2 words <1% mRNA promotes subretinal fibrosis and epithelialmesenchymal transition", Journal of Molecular Cell Biology, 2023 Crossref
- topsecretapiaccess.dovepress.com

8 words = < 1%

29 www.klinikaoczna.pl

- 8 words < 1%
- Lijuan Wang, Zhihao Wu, Congcong Zou, Shaoshuai 7 words < 1 % Liang, Yuxia Zou, Yan Liu, Feng You. "Sex-Dependent RNA Editing and N6-adenosine RNA Methylation Profiling in the Gonads of a Fish, the Olive Flounder (Paralichthys olivaceus)", Frontiers in Cell and Developmental Biology, 2020
- Zhenxiang Wang, Hang Chen, Limin Peng, Yujuan  $_{7 \text{ words}} < 1\%$  He, Jingjing Wei, Xiaonan Zhang. " and are differentially methylated in periodontitis in comparison with periodontal health revealed by microarray of human gingival tissue and transcriptomic analysis ", Journal of Periodontal Research, 2023

Crossref

- Fei-Hong Ji, Xing-Hao Fu, Guo-Quan Li, Qi He, Xin-Guang Qiu. "FTO Prevents Thyroid Cancer Progression by SLC7A11 m6A Methylation in a Ferroptosis-Dependent Manner", Frontiers in Endocrinology, 2022

  Crossref
- Jun Yang, Jingshu Liu, Shaozhen Zhao, Fang Tian. "N6-Methyladenosine METTL3 Modulates the Proliferation and Apoptosis of Lens Epithelial Cells in Diabetic Cataract", Molecular Therapy Nucleic Acids, 2020 Crossref
- Xianying Lu, Wenting Ji, Dingxi Bai, Chenxin Wu, Mingjin Cai, Wei Wang, Chaoming Hou, Jing Gao.

  "Study on the action mechanism of the Fujin Shengji (FJSJ)

  Powder on diabetic ulcer based on network pharmacology and molecular docking", Research Square Platform LLC, 2022

  Crossref Posted Content

OFF

OFF

EXCLUDE QUOTES OFF EXCLUDE BIBLIOGRAPHY OFF EXC